Distant-Neighbor Exchange Constants in Dilute Magnetic Semiconductors

V. Bindilatti, E. ter Haar, and N. F. Oliveira, Jr.
Instituto de Física, Universidade de São Paulo, C.P. 66.318, 05315-970 São Paulo, São Paulo, Brazil

Y. Shapira and M. T. Liu
Department of Physics and Astronomy, Tufts University, Medford, Massachusetts 02155
(Received 18 December 1997)

Several exchange constants J_i between Mn^{2+} ions which are not nearest neighbors were determined in $Zn_{1-x}Mn_xX$ (X = S, Se, Te) from magnetization steps at 20 mK. When the J_i's are listed in order of decreasing size, ratios between successive J_i's are material dependent, and differ from all predictions. The measured J_i's were identified by comparing the magnetization curves with simulations which assumed a random Mn distribution. Contrary to existing theories the second-largest exchange constant is not J_2 between next-nearest neighbors. The most likely alternative is J_4, between fourth neighbors. [S0031-9007(98)06413-8]

PACS numbers: 75.30.Et, 75.50.Ee, 75.50.Pp, 75.60.Ej

The distance dependence of the *d-d* exchange constants J_i in dilute magnetic semiconductors (DMS's) has been discussed for more than a decade [1–9]. The focus has been on Mn-based II-VI DMS's with the zinc-blende structure. It has been established that the largest J_i is the nearest-neighbor (NN) exchange constant J_1. This J_1 is antiferromagnetic (AF), and is of order -10 K [5,6]. It is generally accepted that the second-neighbor (next-nearest-neighbor) exchange constant J_2, third-neighbor constant J_3, etc., are all AF. What is at issue are the ratios $J_1 : J_2 : J_3 : J_4$, etc.

All existing theories, conjectures, and reported data as interpreted by their authors maintain that J_2 is the second-largest exchange constant, after J_1. The theory of Larson *et al.* [1] predicts that $J_2 : J_1$, $J_3 : J_2$, and $J_4 : J_3$ are all about 0.08. In the modified version by Rusin [9], $J_2 : J_1 \cong 0.08$, and both J_3 and J_4 are less than $0.1J_2$. According to Bruno and Lascaray (BL), $J_3 : J_2 = J_4 : J_3 = 1/2$ (no prediction for $J_2 : J_1$) [4]. A power law dependence of J_i on distance, $J_i \propto r_i^{-n}$, was suggested on empirical grounds [3,6]. Quoted values $n \cong 7$ for Mn-based II-VI DMS's imply that $J_2 : J_1 \cong 0.09$, $J_3 : J_2 \cong 0.24$, and $J_4 : J_3 \cong 0.37$.

Most experimental values of J_i other than J_1 were based on quantities which depend on a combination of exchange constants. The extraction of individual J_i involved unverified assumptions concerning the distance dependence of J_i. An example is the analysis of exchange striction [8] in which the BL suggestion $J_3 : J_2 = J_4 : J_3 = 1/2$ is one of the assumptions.

Individual AF exchange constants can be determined directly by the magnetization-step (MST) method [5]. In early works, MST's from NN pairs (J_1 pairs) were used to determine J_1. Later, Larson *et al.* suggested that MST's arising from J_2 pairs, J_3 pairs, etc., can be used to determine these distant-neighbor (DN) J_i's [2]. Because all DN J_i's are $\ll J_1$, much lower temperatures T are required. MST's from DN pairs were observed in Co-based DMS's, which have relatively large J_i [7], but not in Mn-based DMS's on which theoretical efforts have focused.

In this Letter we report direct measurements of distant-neighbors J_i's in $Zn_{1-x}Mn_xX$ (X = S, Se, Te), using MST's at 20 mK. The findings show three major disagreements with all predictions: (1) When the J_i's are listed in order of decreasing size, ratios between successive J_i's are material dependent; (2) numerically, the ratios differ (sometimes widely) from predicted values; (3) identification of the measured J_i, using simulations, indicates that J_2 is not the second-largest J_i, after J_1. The third disagreement hinges on the assumption of a random Mn distribution, but the first two disagreements do not.

Measurements of J_i's are based on the following principles. For low x the dominant features of the magnetization curve arise from singles (isolated spins), and various spin pairs involving different J_i's [7]. At low T the singles lead to a fast rise of the magnetization M at low magnetic fields H. This fast rise is followed by several series of MST's from pairs with different J_i. For pairs consisting of two Mn^{2+} ions there are five MST's in each series at $H_n = 2n|J_i|/g\mu_B$ ($n = 1, 2, \ldots, 5$) [10]. MST's series from successively larger J_i occur at successively higher field ranges, but these field ranges can partially overlap. The exchange constant for any series is obtained from the fields H_n at the MST's and the known g factor (2.0 for Mn^{2+}) [5]. A broadening of the MST's, due to finite T, for example, may cause the MST's in a given series to coalesce and form a "ramp." The field where the ramp ends can be used to estimate the relevant J_i [11].

All samples were melt grown. The Mn concentrations x were deduced from the apparent ("technical") saturation magnetization M_s [5], obtained from 2 K data to 55 kOe (SQUID magnetometer) and 0.6 K data to 180 kOe

(vibrating sample magnetometer). Magnetization measurements at 20 mK used a force magnetometer operating in a plastic dilution refrigerator installed in 50- and 90-kOe superconducting magnets [12].

In the present set of materials the first MST from J_1 pairs occurs well above 100 kOe. Magnetization data at 0.6 K up to 180 kOe (many shown in Ref. [13]), and pulsed-field data [14], indicate that above 70 kOe there are no MST's or ramps from any pairs other than J_1 pairs. The present 20 mK work shows that there are no MST's from pairs between 50 and 70 kOe. (At least one sample from each of the three $Zn_{1-x}Mn_xX$ systems was measured in this range.) Thus, the J_i obtained here from MST's below 50 kOe are the largest J_i except for J_1.

Figure 1(a) shows 20 mK magnetization data for $Zn_{1-x}Mn_xS$. The magnetization ramp ending slightly above 30 kOe corresponds to the largest exchange constant after J_1. The value $J/k_B = -0.41 \pm 0.01$ K is based on the four large dM/dH peaks in Fig. 1(b), located at the 2nd through 5th steps in this series. The first step, near 6 kOe, appears as a structure in the dM/dH curve for the lower x. A change in the slope of the magnetization curves near 20 kOe signals the end of another magnetization ramp. The relevant J is obtained from the small reproducible dM/dH peak at 15.8 kOe, identified as the 4th step in this series. It gives $J/k_B = -0.265 \pm 0.01$ K. The second step in this series, near 8 kOe, leads to a "shoulder" in the dM/dH curves. Yet another magnetization ramp ends near 3 kOe, which gives $J/k_B \cong -0.04$ K. The NN exchange constant, as determined from MST's, is $J_1/k_B = -16.9$ K [14].

The observed ratio $R_{2,1} = 0.41/16.9 = 0.024$ between the second-largest and largest J_i's in $Zn_{1-x}Mn_xS$ is much smaller than the predicted values 0.08 or 0.09 [1,3,6,9]. The observed ratio $R_{3,2} = 0.265/0.41 = 0.65$ between the third-largest and second-largest J_i is much larger than in these theories, but is not far from the BL ratio 1/2. However, the BL ratio 1/2 between the fourth- and third-largest J_i's is much larger than the observed $R_{4,3} \cong 0.15$.

Figure 2(a) shows the upper part of the 20 mK magnetization curves for $Zn_{1-x}Mn_xSe$. There is an obvious ramp which ends near 32 kOe. The four prominent dM/dH peaks in Fig. 2(b) give the second-largest exchange constant $J/k_B = -0.43 \pm 0.01$ K. The leading exchange constant, as obtained from MST's, is $J_1 = -12.2$ K [14]. The observed ratio $R_{2,1} = 0.43/12.2 = 0.035$ is much smaller than all predictions, and is 45% higher than $R_{2,1}$ for $Zn_{1-x}Mn_xS$. Thus, ratios of exchange constants are material dependent.

Among the four prominent peaks in Fig. 2(b) the one near 13 kOe is much larger. The reason is that the 5th peak from the series associated with the third-largest J_i is practically at the same field. The small, but reproducible, dM/dH peak at 9.7 kOe is the 4th step in this new series. It gives $J/k_B = -0.163 \pm 0.01$ K. At still lower fields, the fourth-largest exchange constant $J/k_B \cong -0.07$ K leads to a ramp which ends near 5.5 kOe. This ramp is more obvious when the ordinate scale in Fig. 2(a) starts from zero.

Figure 3 shows the upper part of the 20 mK magnetization curves for $Zn_{1-x}Mn_xTe$. A ramp ending near 40 kOe

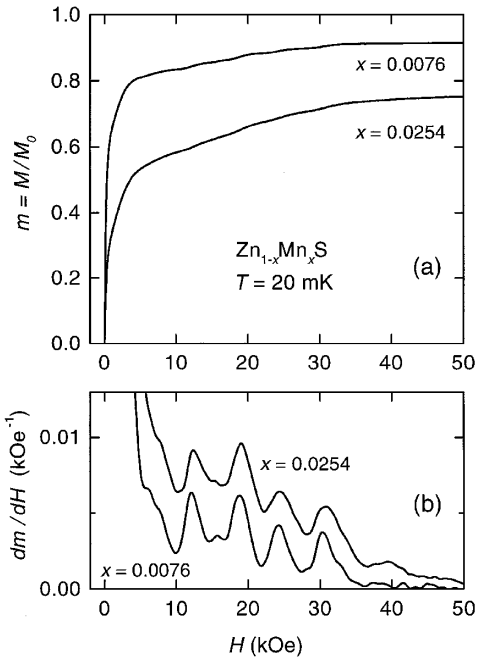

FIG. 1. (a) Observed magnetization of $Zn_{1-x}Mn_xS$ at 20 mK. In all figures, the magnetization M is corrected for lattice diamagnetism, and is normalized to the calculated true saturation value M_0 (all spins fully aligned). (b) Field derivative of the observed normalized magnetization $m = M/M_0$.

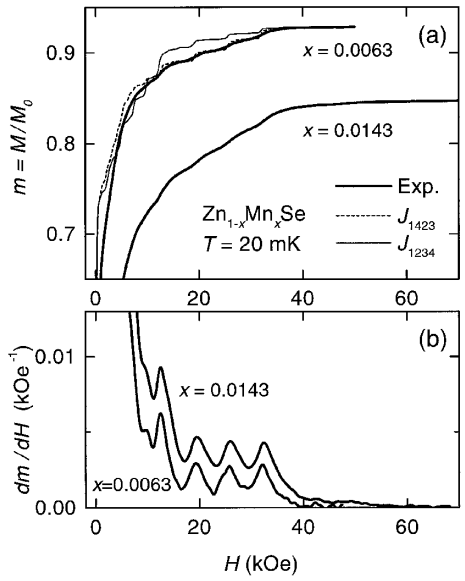

FIG. 2. (a) Observed magnetization for $Zn_{1-x}Mn_xSe$ at 20 mK. Also shown are the J_{1423} and J_{1234} simulations for $x = 0.0063$. (b) The derivative dm/dH of the experimental curves.

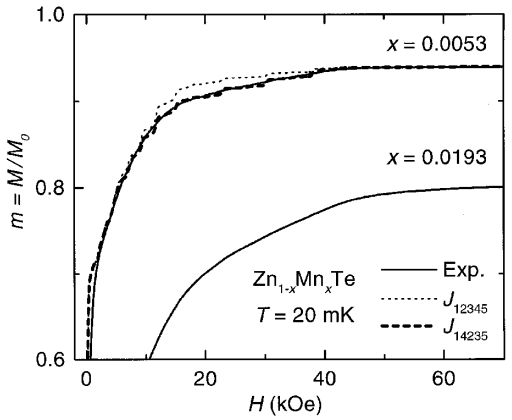

FIG. 3. Magnetization curves for $Zn_{1-x}Mn_xTe$ at 20 mK. Also shown are the simulation J_{12345} and J_{14235} for $x = 0.0053$.

is clearly visible. The derivative dM/dH for $x = 0.0053$ (not shown) reveals three broad steps in this series, which give $J/k_B = -0.51 \pm 0.03$ K for the second-largest J_i. Between 5 and 12 kOe the derivative reveals four steps of another series, with $J/k_B = -0.16 \pm 0.02$ K. The largest exchange constant is $J_1/k_B = -9$ K [14–16]. Thus, $R_{2,1} = 0.51/9 = 0.06$, which is more than twice the ratio for $Zn_{1-x}Mn_xS$.

Extensive simulations of the magnetization curves were performed in order to identify the particular distant neighbor i responsible for each measured J_i. The simulations used standard cluster models [7], but the assumption that the J_i's decrease monotonically with r_i was relaxed. Instead, alternative sequences of the J_i's in terms of size were attempted, to optimize the match with the data. The simulations included J_1 through J_4, or J_1 through J_5. The notation J_{jklm} means that the simulation assumes $|J_j| > |J_k| > |J_l| > |J_m|$.

The simulations included singles, and the various types of pairs, triplets, and quartets [13]. With four or five J_i's there are hundreds of quartet types. The magnetization of each cluster type was obtained via the partition function following a diagonalization of the Heisenberg Hamiltonian. The total magnetization M was then constructed using the probabilities for finding each cluster type. The probabilities were obtained from a computer program, more general than in Refs. [13] and [17]. The key assumption was that the Mn ions were randomly distributed.

ZnTe and ZnSe have the zinc-blende structure, but ZnS has many polytypes with stacking sequences ranging from zinc blende to wurtzite [18]. For our $Zn_{1-x}Mn_xS$ samples the x-ray powder patterns were nearly identical to the zinc-blende pattern, but very different from wurtzite. Therefore, the cluster statistics was always for the zinc-blende structure (fcc cation lattice).

The simulations neglected clusters with more than four spins. Because this approximation holds only for low x, the identification of the J_i's was based on comparisons with data for $x < 0.008$. Simulations with different sequences of J_i's produce very different magnetization curves essentially because of the very different sizes of MST's (or ramps) arising from different pairs. In the fcc cation lattice there are 6, 24, and 12 second, third, and fourth neighbors, respectively.

Three of the six possible simulations for $Zn_{1-x}Mn_xS$ are shown in Fig. 4 [19]. The simulation J_{1234}, with $|J_1| > |J_2| > |J_3| > |J_4|$, is in poor agreement with the data. The predicted change of slope near 30 kOe, which in this simulation is mainly due to the end of the ramp from J_2 pairs, is too small. The predicted change of slope near 20 kOe (end of ramp from J_3 pairs) is far too large. These discrepancies for sudden changes of slope cannot be explained by the neglect of J_i's beyond J_4. The simulation J_{1243} still underestimates the slope just below 30 kOe, and overestimates the change of slope near 20 kOe. The best agreement is with the simulation J_{1423}, based on the assignments $J_4/k_B = -0.41$ K, $J_2/k_B = -0.265$ K, and $J_3/k_B \cong -0.04$ K [20]. The three simulations not shown in Fig. 4 (J_{1324}, J_{1342}, and J_{1432}) are in very poor agreement with the data.

Two of the six simulations for $Zn_{1-x}Mn_xSe$ with $x = 0.0063$ are shown in Fig. 2(a). The simulation J_{1234} again grossly underestimates the change of slope near 32 kOe. Thus, the second-largest exchange constant cannot be J_2. The simulations J_{1243}, J_{1432}, J_{1324}, and J_{1342} (not shown) are also in poor agreement with the data. Only the J_{1423} simulation fits the data reasonably well [21]. On this basis, $J_4/k_B = -0.43$ K, $J_2/k_B = -0.163$ K, and $J_3/k_B \cong -0.07$ K.

The simulations for $Zn_{1-x}Mn_xTe$ with $x = 0.0053$ again indicate that the second-largest J_i (-0.51 K) is not J_2 but is most likely J_4. The simulations strongly suggest that the exchange constant -0.16 K, observed at lower fields, is J_3. Although no other MST's or obvious ramps

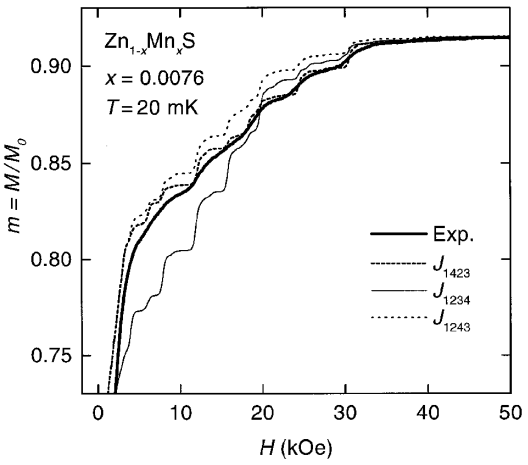

FIG. 4. Comparison between the observed normalized magnetization m for $Zn_{1-x}Mn_xS$ ($x = 0.0076$) and three simulations which include J_1 through J_4. The notation J_{jklm} means that $|J_j| > |J_k| > |J_l| > |J_m|$.

TABLE I. Exchange constants J_i/k_B (K) with the present assignments. Values of J_1 are from Refs. [14–16]. Values in parentheses are tentative.

Material	J_1/k_B	J_2/k_B	J_3/k_B	J_4/k_B	J_5/k_B
$Zn_{1-x}Mn_xS$	−16.9	−0.27	−0.04	−0.41	···
$Zn_{1-x}Mn_xSe$	−12.2	−0.16	−0.07	−0.43	···
$Zn_{1-x}Mn_xTe$	−9	(−0.2)	−0.16	−0.51	(−0.07)

were observed in the data, much closer agreement with the data was obtained when the simulations also included $J_2/k_B \cong -0.2$ K and $J_5/k_B \cong -0.07$ K. The simulations J_{14235} and J_{12345} shown in Fig. 3 are based on these exchange constants. Clearly, J_{14235} is superior. The experimental observation of MST's (or ramp) from the J_2 pairs is difficult in this material because $J_2 \cong J_3$ and the steps (ramp) from the J_3 pairs are much larger. J_5 was needed to improve the agreement below a few kOe. The results for J_2 and J_5 are much less certain than those for J_4 and J_3.

The results for the J_i's in all materials are summarized in Table I. The simulations used to identify the J_i assumed a random Mn distribution in Mn-based DMS. There is strong experimental evidence for this assumption [5]. It includes the apparent saturation value (essentially the number of singles), the size of MST's from J_1 pairs (number of NN pairs), and the proportionality between the Curie-Weiss θ and x. The chance that all present samples are abnormal, having a nonrandom Mn distribution with a number of J_2 pairs which just happens to match the number of J_4 pairs for a random distribution, seems remote. Thus, it is very unlikely that a nonrandom distribution led to a misidentification of the J_i's. Supporting evidence for a large J_4 also comes from a recent neutron-diffraction determination of the AF structure of a related material [22]. Finally, major disagreements with existing theories remain irrespective of the identities of the J_i's.

We are grateful to A. Twardowski for several samples, and to S. Morelhão for x-ray work. This work was supported by FAPESP, FINEP, and CNPq. Travel funds for Y. S. were provided by the University of S. Paulo.

[1] B. E. Larson, K. C. Hass, H. Ehrenreich, and A. E. Carlsson, Phys. Rev. B **37**, 4137 (1988).
[2] B. E. Larson, K. C. Hass, and R. L. Aggarwal, Phys. Rev. B **33**, 1789 (1986).
[3] A. Twardowski, H. J. M. Swagten, W. J. M. de Jonge, and M. Demianiuk, Phys. Rev. B **36**, 7013 (1987).
[4] A. Bruno and J. P. Lascaray, Phys. Rev. B **38**, 9168 (1988).
[5] Y. Shapira, J. Appl. Phys. **67**, 5090 (1990); in *Semimagnetic Semiconductors and Diluted Magnetic Semiconductors*, edited by M. Averous and M. Balkanski (Plenum, New York, 1991).
[6] W. J. M. de Jonge and H. J. M. Swagten, J. Magn. Magn. Mater. **100**, 322 (1991).
[7] T. Q. Vu *et al.*, Phys. Rev. B **46**, 11 617 (1992); Y. Shapira *et al.*, Solid State Commun. **75**, 201 (1990).
[8] Q. Shen, H. Luo, and J. K. Furdyna, Phys. Rev. Lett. **75**, 2590 (1995).
[9] T. M. Rusin, Phys. Rev. B **53**, 12 577 (1996).
[10] All J's are based on an exchange interaction $-2J\mathbf{S}_1 \cdot \mathbf{S}_2$ within a pair.
[11] V. Bindilatti *et al.*, Phys. Rev. B **53**, 5472 (1996); E. ter Haar *et al.*, Phys. Rev. B **56**, 8912 (1997).
[12] V. Bindilatti and N. F. Oliveira, Jr., Physica (Amsterdam) **194-196B**, 63 (1994).
[13] Quartets involving J_1 were discussed by M. T. Liu *et al.*, Phys. Rev. B **54**, 6457 (1996).
[14] S. Foner *et al.*, Phys. Rev. B **39**, 11 793 (1989); Y. Shapira *et al.*, Solid State Commun. **71**, 355 (1989).
[15] J. P. Lascaray *et al.*, Phys. Rev. B **35**, 6860 (1987); G. Barilero *et al.*, Solid State Commun. **62**, 345 (1987).
[16] T. M. Giebultowicz *et al.*, J. Appl. Phys. **67**, 5096 (1990); L. M. Corliss *et al.*, Phys. Rev. B **33**, 608 (1986).
[17] U. W. Pohl and W. Busse, J. Chem. Phys. **90**, 6877 (1989).
[18] W. L. Roth, in *Physics and Chemistry of II-VI Compounds*, edited by M. Aven and J. S. Prener (North-Holland, Amsterdam, 1967).
[19] For $x = 0.0076$ the simulations with J_1 through J_4 include only 98.9% of the spins. The simulations in Fig. 4 include a multiplication by a scale factor 1.012 which brings all these simulations into agreement with the data at the highest field. The scale factors for the simulations in Figs. 2 and 3 are 1.007 and 1.014, respectively.
[20] Additional simulations which include J_5 show that the second-largest J_i cannot be J_5. Basically, the 24 fifth-neighbor cation sites cause the slope of the ramp ending near 30 kOe to be too high.
[21] The slower rise of the experimental curve below ~2 kOe is consistent with the expected effect of J_i's smaller than the four included in the simulation.
[22] T. Fries *et al.*, Phys. Rev. B **56**, 5424 (1997).